Received: 27 February 2018 | Revised: 22 April 2018 | Accepted: 6 May 2018

DOI: 10.1111/pce.13341

ORIGINAL ARTICLE

WILEY Plant, Cell & Environment

Root-expressed phytochromes B1 and B2, but not PhyA and Cry2, regulate shoot growth in nature

Youngjoo Oh[1*] | Variluska Fragoso[1*] | Francesco Guzzonato[1] | Sang-Gyu Kim[1†] | Chung-Mo Park[2] | Ian T. Baldwin[1]

[1] Department of Molecular Ecology, Max Planck Institute for Chemical Ecology, Hans-Knöll-Straße 8, D-07745 Jena, Germany

[2] Department of Chemistry, Seoul National University, Seoul 08826, South Korea

Correspondence
Ian T. Baldwin, Department of Molecular Ecology, Max Planck Institute for Chemical Ecology, Hans-Knöll-Straße 8, D-07745 Jena, Germany.
Email: baldwin@ice.mpg.de

Present Address
[†]Present address of: S-G. K., Department of Biological Sciences, Korea Advanced Institute of Science and Technology, 291 Daehak-ro, Yuseong-gu, Daejeon 34141, Korea.

Funding information
H2020 European Research Council; Max-Planck-Gesellschaft; National Research Foundation of Korea, Grant/Award Number: 2012055546; Human Frontier Science Program, Grant/Award Number: RGP0002/2012; Max Planck Society; European Research Council, Grant/Award Number: 293926

Abstract

Although photoreceptors are expressed throughout all plant organs, most studies have focused on their function in aerial parts with laboratory-grown plants. Photoreceptor function in naturally dark-grown roots of plants in their native habitats is lacking. We characterized patterns of photoreceptor expression in field- and glasshouse-grown *Nicotiana attenuata* plants, silenced the expression of *PhyB1/B2/A/Cry2* whose root transcripts levels were greater/equal to those of shoots, and by micrografting combined empty vector transformed shoots onto photoreceptor-silenced roots, creating chimeric plants with "blind" roots but "sighted" shoots. Micrografting procedure was robust in both field and glasshouse, as demonstrated by transcript accumulation patterns, and a spatially-explicit lignin visual reporter chimeric line. Field- and glasshouse-grown plants with *PhyB1B2*, but not *PhyA* or *Cry2*, -blind roots, were delayed in stalk elongation compared with control plants, robustly for two field seasons. Wild-type plants with roots directly exposed to FR phenocopied the growth of *irPhyB1B2*-blind root grafts. Additionally, root-expressed *PhyB1B2* was required to activate the positive photomorphogenic regulator, *HY5*, in response to aboveground light. We conclude that roots of plants growing deep into the soil in nature sense aboveground light, and possibly soil temperature, via *PhyB1B2* to control key traits, such as stalk elongation.

KEYWORDS

grafting, growth, HY5, light, phytochrome B, roots

1 | INTRODUCTION

Light is both a source of energy for photosynthesis and a crucial environmental signal that controls many photomorphogenic responses including the induction of seed germination, seedling development, such as hypocotyl growth inhibition, cotyledon expansion, promotion of shoot and root growth, and the regulation of photoperiodism (reviewed in Casal, 2013). Photoreceptors are sensitive and dynamic sensors that capture environmental light information such as intensity, quality, direction, and period to rapidly respond and adapt to any given environment fluctuation, optimizing plant growth, and development (reviewed in Endo, Araki, & Nagatani, 2016). Several photoreceptors have been identified, such as UV RESISTANCE LOCUS8 (UVR8), phototropins (Phot), and cryptochromes (Cry) for ultraviolet (UV) and blue light, and the phytochromes (Phy) for red and far-red light perception (reviewed in Galvão & Fankhauser, 2015).

Light quality usually refers to the red (R):far-red (FR) light ratio sensed by the Phys that occur in two photoconvertible forms: Pr (phytochrome red) is the biologically inactive form in which the Phys are synthesized. Upon R exposure, Pr is converted to Pfr (phytochrome far-red), its active form, which moves into the nucleus where it regulates the expression of downstream target genes. Further

[*] Y. O. and V. F. contributed equally to this work.

exposure to FR returns Pfr to Pr, or vice versa by R exposure (Bae & Choi, 2008). Phys are known to be encoded by a small gene family of four clades (PHYA, PHYC, PHYB/D—or the PHYB-clade—and PHYE) in dicotyledonous species, whereas only three (PHYA, PHYC, and PHYB) in monocotyledonous species (Clack, Mathews, & Sharrock, 1994; Mathews & Sharrock, 1997). Recently, Fragoso, Oh, Kim, Gase, and Baldwin (2017) identified five phytochrome members (*NaPhyA*, two members belonging to the *NaPhyB* clade, *NaPhyC*, and *NaPhyE*) in *Nicotiana attenuata*, a native tobacco that has been developed into an ecological expression system and demonstrated some of the distinct, synergistic, and antagonistic functions of the different Phy members in growth and development with phytochrome-silenced *N. attenuata* lines.

ELONGATED HYPOCOTYL 5 (HY5) is a key component of several light signalling pathways that regulate growth and development in response to environmental signals. HY5 functions downstream directly and indirectly in the signalling pathways initiated by multiple photoreceptors and phytohormones and adjusts the expression of many target genes to optimize photosynthetic performance and plant growth. Therefore, HY5 is a signal convergence point for these pathways (Cluis, Mouchel, & Hardtke, 2004; Franklin, Toledo-Ortiz, Pyott, & Halliday, 2014; Lau & Deng, 2010; Lee et al., 2007). In Arabidopsis (*Arabidopsis thaliana*), HY5 is also a shoot-to-root mobile signal that mediates coordinated shoot:root growth by balancing carbon assimilation and nitrate metabolism (Chen et al., 2016). Lastly, root-HY5, activated by root-AtPhyB, modulates root architecture, particularly gravitrophic responses during the early stages of root growth (Lee et al., 2016). These studies suggest that both the mobile shoot-derived HY5 and local root-HY5 mediate the light-responsive regulation of whole-plant growth in Arabidopsis.

Light perception, the downstream signalling pathways and the physiological responses mediated by photoreceptors have been thoroughly studied (Christie, Blackwood, Petersen, & Sullivan, 2015; Franklin & Quail, 2010; Tossi, Lamattina, Jenkins, & Cassia, 2014). Earlier studies that attempted to understand the tissue- or organ-specific light responses of photoreceptors were conducted with a localized (microbeam) irradiation restricted to a particular tissue or organ of a seedling, a dissected tissue, or isolated parts, such as fruits. As molecular biology techniques improved, tissue-specific promoters were used to dissect the distinct functions of photoreceptors in shoot and root development (reviewed in Montgomery, 2016). However, most studies focused on the functions of photoreceptors in aboveground tissues, as if photoreceptors only function in tissues directly exposed to light. Yet, in many plant species, it is known that photoreceptors are highly expressed in roots, which are in a relatively dark underground environment (Adam, Kozma-Bognar, Schafer, & Nagy, 1997; Goosey, Palecanda, & Sharrock, 1997; Sharrock, 2002; Somers & Quail, 1995a, 1995b), and root-photoreceptors also have been shown to be directly or indirectly activated by aboveground light piped through the vascular tissues (Lee et al., 2016; Mandoli & Briggs, 1982; Sun, Yoda, & Suzuki, 2005; Sun, Yoda, Suzuki, & Suzuki, 2003) or soil (Ciani, Goss, & Schwarzenbach, 2005; Mandoli, Ford, Waldron, Nemson, & Briggs, 1990; Tester & Morris, 1987). Aboveground light is well known to dramatically influence a broad spectrum of root growth, development, behavior, and also circadian period of root tissue (Lee, Park, Ha, Baldwin, & Park, 2017; Mo, Yokawa, Wan, & Baluška, 2015; Nimmo, 2018), but this work has been performed with seedlings, grown under the controlled conditions of agar-plate culture system in which both shoots and roots are illuminated and/or subjected to spectrally depauperate light (Correll & Kiss, 2005; Costigan, Warnasooriya, Humphries, & Montgomery, 2011; De Simone, Oka, & Inoue, 2000; Dyachok et al., 2011; Salisbury, Hall, Grierson, & Halliday, 2007). Many studies do not include the photomorphogenic-relevant light spectra, providing plants with only those wavelengths that are directly translated into chemical energy via photosynthesis (400–700 nm: photosynthetically active radiation [PAR]). However, plants have evolved photoreceptors, capable of sensing and triggering physiological adaptations to a wider range of light wavelengths, which includes the UV (100 to 400 m) and the far-red light (FR, 710 to 800 nm). Recently, studies also have emphasized that laboratory experiments with plants grown under non-natural light condition often lead to physiological and morphological artifacts that can confound functional interpretations (Brachi et al., 2010; Lekberg & Helgason, 2018; Novák et al., 2014; Poorter et al., 2016; Xu et al., 2013; Yokawa, Fasano, Kagenishi, & Baluška, 2014). Moreover, as sunlight radiation combines light and heat, the recent discovery that phytochromes also enable plants to respond to temperature changes is perhaps not surprising (Jung et al., 2016; Legris et al., 2016). Phytochromes clearly help plants optimize their growth and development, particularly in establishing flowering times that maximize reproductive success (Fitter & Fitter, 2002; Lumsden 2002; Blázquez, Ahn, & Weigel, 2003). Therefore, it remains unclear how well results from experiments conducted during the early developmental stages of plants grown under controlled laboratory or growth chamber conditions apply to mature adult plants grown in their natural habitats. Thus, we are still in the early stages in understanding how photoreceptors allow plants to optimize their growth in nature.

In order to understand the ecologically relevant functions of root-expressed photoreceptors, particularly those of the phytochrome B clade (*NaPhyB1* and *NaPhyB2*), in whole-plant growth and development, we created chimeric plants with "sighted" shoots and "blind" roots using a micrografting technique and examined these micrografted individuals through all stages of development in both the glasshouse and in a nature preserve in the plant's native habitat.

2 | MATERIALS AND METHODS

2.1 | Plant transformation

To generate stably-silenced *NaCry2*, or *NaPhyB1B2* transgenic lines, gene-specific fragments of *NaCry2* (locus_tag = "A4A49_43524") or of a consensus region of both *NaPhyB1* and *NaPhyB2* (Table S1) were cloned into transformation vectors (pRESC8:*NaCry2*, Figure S1a; and pSOL8DC7:*NaPhyB1B2*, Figure S1d) as inverted repeats (ir) driven by the CaMV 35S promoter, respectively, and each of these constructs, along with an empty vector (WT plants transformed with an empty vector construct as control, pSOL3NC), were transformed into *N. attenuata* wild-type plants (from the 31st inbred generation of *N. attenuata* seeds originally collected at the Desert Inn Ranch in Utah,

USA, in 1988) using the LBA4404 strain *Agrobacterium tumefaciens*-mediated transformation (Krügel, Lim, Gase, Halitschke, & Baldwin, 2002). Two independently transformed stably-silenced lines of *irCry2* (*irCry2-282-3-9* and *irCry2-318-4-2*) and one of *irPhyB1-B2* (*irPhyB1-B2-150-6*) were screened and selected according to Gase, Weinhold, Bozorov, Schuck, and Baldwin (2011). Homozygous transgenic lines met the requirements of homozygosity, as confirmed by 100% hygromycin resistance, diploidy, as measured by flow cytometry, and single, full T-DNA integrations into the genome as verified by diagnostic PCRs and Southern blotting, respectively (Figure S1). The absence of off-target effects of the sequence fragments used to generate the transgenic lines was verified using an in-house *N. attenuata* virus-induced gene silencing (VIGS) tool constructed from the Sol Genomics Network (SGN) virus-induced gene silencing tool designed for the Solanaceae family (http://vigs.solgenomics.net/), but using the *N. attenuata* genome (Xu et al., 2017) as the database. Additional stably-silenced lines were used and previously characterized by Fragoso et al., 2017, namely, lines silenced for *NaPhyA* (*irPhyA-200* and *irPhyA-213*) and crosses made with lines individually silenced for *NaPhyB1* and *NaPhyB2*, leading to the hemizigous *irPhyB1xB2* lines *irPhyB1-178* × *irPhyB2-204* and *irPhyB1-246* × *irPhyB2-171*.

2.2 | Plant growth conditions

N. attenuata seeds were sterilized and germinated on Petri dishes with Gamborg's B5 media (Duchefa) as described in Krügel et al. (2002). Seed-containing Petri dishes were kept in growth chambers (Percival, Perry, IA, USA) under 16-hr light/8-hr dark regime for an initial 3 days at 30 ± 2 °C, and then at 26 ± 2 °C. Approximately 7 days after germination, micrografting was performed on 0.8% plant agar containing Gamborg's B5 media (Duchefa) in a sterile bench with an Olympus SZ51 stereomicroscope as described in Fragoso, Goddard, Baldwin, and Kim (2011). Grafted seedlings were grown in a growth chambers (Percival, Perry, IA, USA) under 16-hr light/8-hr dark regime for 26 ± 2 °C. Approximately 7–10 days after grafting, successfully grafted seedlings were transferred into Teku pots (Poppelmann GmbH & Co. KG, Lohne, Germany) for an additional 10–12 days, followed by a final transfer into individual 1-L pots in the glasshouse under 16 hr of natural daylight supplemented by Philips Master Sun-T PIA Agro 400 or 600-W sodium lights at 23–25 °C, and 8 hr of dark at 19–23 °C and 45% to 55% relative humidity.

For the release of transgenic plants at the Utah field station, we germinated empty vector (EV, pSOL3NC) and *irPhyB1-B2* seeds on Gamborg's B5 medium as described above, and approximately 10 days after germination, micrografting were performed on 1.0% plant agar containing Gamborg's B5 media (Duchefa) on the working bench under with a stereo microscope and kept at room temperature under 16-hr light/8-hr dark conditions for another 10–15 days. Successfully grafted seedlings were transferred to prehydrated 50-mm peat pellets (Jiffy 703; http://www.jiffypot.com), and gradually adapted to the high light and low relative humidity of the Great Basin Desert over a 2-week period. Finally, preadapted rosette-stage plants were transplanted into a field plot and watered until the roots had become established, and the plants were able to grow without water supplementation. The transgenic seeds were imported under U.S. Department of Agriculture Animal and Plant Health Inspection Service permit number 07-341-101n and released under notification numbers 11-350-101r in 2012 and 12-333-101r in 2013, respectively.

To monitor the growth and development of grafts, we measured growth parameters such as rosette size and stalk length on a weekly basis from early rosette stage (36 days after germination [DAG] for glasshouse-grown plants, and 21 days after planting in experimental plot for field-grown plants) to the late flowering stage (64 DAG for glasshouse-grown plants, and 32 days after planting in experimental plot for field-grown plants).

2.3 | RNA extraction and gene expression

Total RNA was extracted from approximately 100 mg of frozen leaf and root tissues with Trizol reagent, followed by DNase-I treatment (Fermentas) according to the manufacturer's instructions. Remaining DNase was removed by phenol extraction and precipitated with addition of 3-M sodium acetate (pH 5.2) and pure ethanol. The cDNA was synthesized using RevertAidTM H Minus reverse transcriptase (Fermentas) and oligo dT primer (Fermentas) from 1 μg of total RNA measured by a NanoDrop ND-1000 spectrophotometer (NanoDrop Technologies, Wilmington, DE, USA). Quantitative RT-PCR (qPCR) analyses were performed on a Stratagene MX3005P (Agilent Technologies, Santa Clara, CA, USA) using a core reagent kit for SYBR Green I (Eurogentec) and gene-specific primer pairs (Table S2). Relative transcript accumulation was calculated from calibration curves obtained from the analysis of dilution series of cDNA samples, and the values were normalized by the expression of housekeeping gene *NaEFα1* (*N. attenuata elongation factor alpha 1*). All reactions were performed using the following qPCR conditions: initial denaturation step of 95 °C for 30 s, followed by 40 cycles each of 95 °C for 30 s, 60 °C for 30 s, and 72 °C for 1 min, followed by melting curve analysis of PCR products.

2.4 | Light treatments

To investigate whether light signalling in the roots is induced by aboveground light, 35-day-old sand-grown plants were moved from the glasshouse into two climate chambers, both with normal light/dark cycle (lights on at 06:00 hr, and lights off at 22:00 hr, fluorescence lamp in the climate chamber, ≈294 $\mu mol \cdot m^{-2} \cdot s^{-1}$ PAR). Next morning, we extended the dark period of one chamber, which housed the control plants, and we performed the light treatment from 06:00 to 07:00 hr for the plants of the second chamber. Then, at 07:00 hr, leaves and roots of plants of both light and dark treatments were quickly collected and frozen at −80 °C until further analysis. Plants of the dark treatment were collected under dim green light.

For root-FR treatments, 5-W FR light-emitting diodes (LEDs; 720 ± 10 nm) were connected to fibre-optic cables and placed at the upper 1 cm of the roots, just below the soil surface, to trigger light-mediated signalling in the roots (Figure S2). In an attempt to phenocopy, the EV/*irPhyB1xB2* grafts, which have constantly inactive PhyB in the roots, the FR root exposure started at an early growth stage (25-day-old soil-grown plants) and continued throughout the light period (6:00 to 22:00 hr) of the light:dark cycles. As controls, plants were either kept under normal ambient light conditions (approximately 528 $\mu mol \cdot m^{-2} \cdot s^{-1}$ PAR and R: FR ratio = 2.0) or

supplemented with shoot-FR (approximately 528 μmol·m^{-2}·s^{-1} PAR and R: FR ratio = 0.5) using the 5-W FR LEDs (720 ± 10 nm, fluence rate: ≈80 μmol·m^{-2}·s^{-1} at 1-cm distance from the lens) placed on aluminium blocks directed towards the top of the shoots (6 to 22 hr, Figure S2). The light treatments were maintained until plants were in the early flowering stage (~35 days after the start of FR treatment), and leaf and root samples were collected at the early elongation stage (14 days after the start of FR treatment, at 7:00 a.m.) to analyse the transcripts levels related to FR signalling. Light quality and quantity in both glasshouse and field were measured by a spectroradiometer, JETI Specbos 1211(JETI Technische Instrumente GmbH, Jena, Germany).

2.5 | Statistical analysis

Data were analysed with SigmaPlot 12.0 software (Systat Software Inc., https://systatsoftware.com) using appropriate methods (e.g., Student's *t* tests for paired comparisons and one or two-way analyses of variance (ANOVAs) followed by Fisher LSD, Dunn's, Tukey, or Student–Newman–Keuls as post hoc tests for multiple comparisons).

3 | RESULTS AND DISCUSSION

3.1 | Photoreceptors are expressed throughout *N. attenuata* plants

We examined the transcript accumulations of seven key photoreceptors (i.e., *NaUVR8*, *NaPhot1*, *NaCry1*, *NaCry2*, *NaPhyA*, *NaPhyB1*, and *NaPhyB2*) in *N. attenuata* plants naturally growing in their native habitat, the Great Basin Desert, Utah, USA (Figure 1a, left panel) with full spectrum of strong light (Figure 1a, lower right panel; irradiance: 565.8 W/cm^2; PAR: 1858.80 μmol·m^{-2}·s^{-1}). Considering naturally grown *N. attenuata* root architecture (Figure 1a, upper right panel), 17 different aboveground and belowground tissues, from flower buds to root tips including lateral roots, were sampled (Figure 1b), and the tissue-specific photoreceptor transcript accumulations among those tissues was measured (Figure 1c). Most of the transcripts analysed were highly expressed throughout all tissues, including the roots, which were growing deep into the soil, and were competely in the dark (Figure 1c). Interestingly, the transcript levels of *NaPhyA* and *NaCry2* were higher in roots than in the shoots, whereas the levels of *NaUVR8*, *NaCry1*, *NaPhyB1*, and *NaPhyB2* in the roots were comparable to those found in aerial plant parts (Figure 1c).

Although the main goal of this present study was to understand the ecological functions of root-photoreceptors in nature, glasshouse experiments are also valuable as they reduce the scale of the environmental variations found in the field to the most essential and critical manipulations necessary to falsify specific hypothesis regarding gene function. Differences were obvious when comparing field- versus glasshouse-grown plants, such as root architecture, roots growing deep into dark soil (as opposed to roots growing in shallow pots with holes at the bottom through which light can be perceived), soil nutrient availability, and ambient light spectra (Figures 1a and S3a). However, the overall patterns of transcript accumulation in aboveground and belowground tissues of the glasshouse-grown plants were

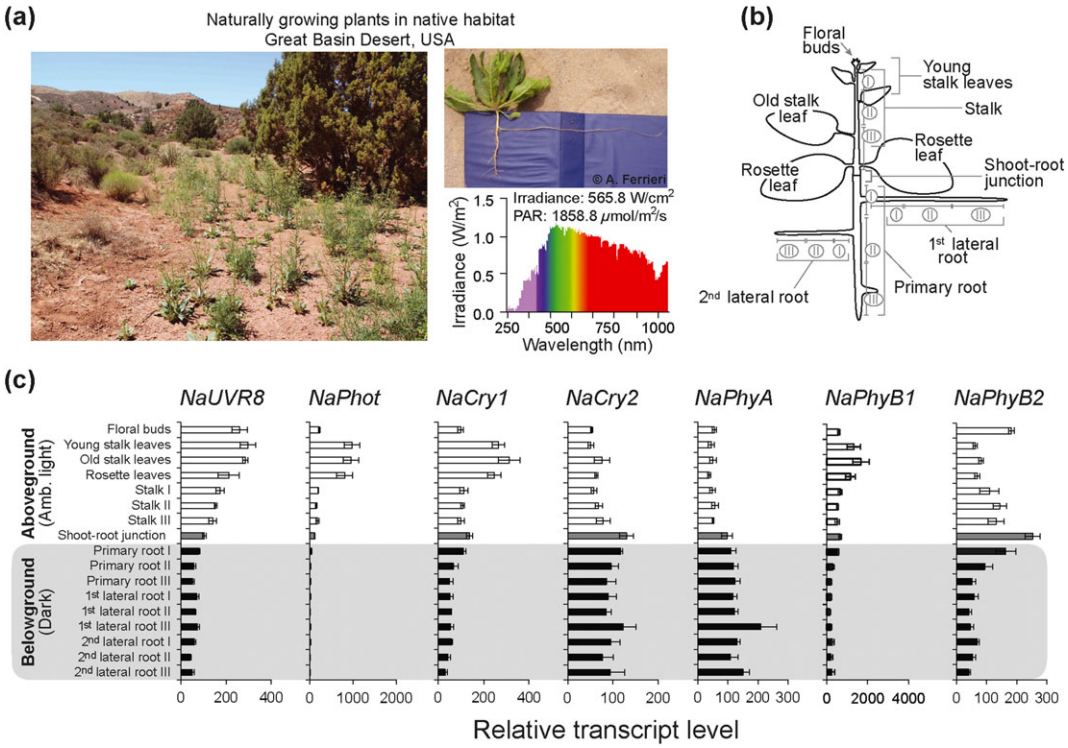

FIGURE 1 Transcript levels of photoreceptors in plant organs dissected from *N. attenuata* growing in nature. (a) *N. attenuata* plants naturally growing in their native habitat, the Great Basin Desert, Utah, USA (shown in left), under sunlight (solar spectra shown in bottom right). Plants were excavated (shown in upper right) and analysed in (b) 17 different plant parts regarding the (c) relative transcript accumulation of each photoreceptor, measured by quantitative real-time PCR (qPCR). Bars indicate *EF1a*-normalized relative transcript levels of target genes ±SE (n = 5). See Figure S3 for a similar analysis of glasshouse-grown plants

consistent with data from plants growing in their native environment (Figures 1c and S3c). Notably, the transcript levels of *NaPhyA*, *NaPhyB2*, and *NaCry2* in roots were either higher or comparable with those found in shoots (Figures 1c and S3c).

Based on the patterns of transcript accumulations found in both native and glasshouse-grown *N. attenuata* plants, we selected four photoreceptors, *NaPhyA*, *NaPhyB1*, *NaPhyB2*, and *NaCry2*, whose transcripts were highly accumulated in belowground parts for further functional analysis in the context of whole-plant growth and development.

3.2 | Generation of photoreceptor-silenced transgenic plants

To investigate the specific functions of root-expressed photoreceptors in plant growth and development, we used inverted-repeats (ir) transgenic plants stably silenced for *NaPhyA* (*irPhyA*), for *NaPhyB1B2* (the hemizigous cross *irPhyB1xB2*, and the homozygous *irPhyB1-B2*—we used plants cosilenced in both *NaPhyB1* and *NaPhyB2* expression to cover for any potential redundancy amongst the members of the closely related phytochrome B clade), and for *NaCry2* (*irCry2*). The transgenic lines silenced individually for *NaPhyA* (*irPhyA*), *NaPhyB1* (*irPhyB1*), and *NaPhyB2* (*irPhyB2*), together with the hemizigous line silenced for both *NaPhyB1* and *NaPhyB2* created by reciprocal *irPhyB1* and *irPhyB2* crossings (*irPhyB1xB2*), were previously characterized and published (Fragoso et al., 2017). *irPhyA* plants showed 80% reductions in *NaPhyA* transcript accumulations compared with those of EV plants, and *irPhyB1xB2* plants showed 54% reductions in *NaPhyB1* and 70% in *NaPhyB2* transcript accumulations compared with those of EV plants (see Fragoso et al., 2017).

Additionally, we transformed *N. attenuata* plants with RNAi vectors harboring sequence fragments specific to *NaCry2* (pRESC8CRY2), or to a consensus region of both *NaPhyB1* and *NaPhyB2* (pSOL8DC7, Table S1). Homozygous lines of *irCry2* and *irPhyB1-B2* were generated and screened according to Gase & Baldwin, 2012 (Figure S1). Three independently transformed lines for each transformation vector were selected that harbored a single-copy insertion of the T-DNA and for which T_2 plants showed significant reductions in transcript accumulations of the target gene(s). The single copy insertion of constructs of both lines, *irCry2* and *irPhyB1-B2*, was confirmed by Southern blotting (Figure S1b,e), and the silencing efficiency of *NaCry2* in *irCry2* lines and of *NaPhyB1* and *NaPhyB2* in *irPhyB1-B2* lines was measured by qPCR (Figure S1c,f). All four tested *irCry2* plants showed approximately 85% and 30% reductions of *NaCry2* and *NaCry1* transcript accumulation, respectively, compared with empty vector (EV) control plants (Figure S1c), and the transgenic line 150-6 of *irPhyB1-B2*-silenced plants showed 68% and 81% reductions in *NaPhyB1* and *NaPhyB2* transcript accumulations, respectively, compared with EV plants, while retaining EV levels of *NaPhyA*, *NaPhyC*, and *NaPhyE* transcripts (Figure S1f). Most importantly, the strong constitutive shade-avoidance responses that characterize phytochrome-deficient plants (Devlin et al., 1999; Fragoso et al., 2017; Reed, Nagpal, Poole, Furuya, & Chory, 1993; Weller, Schreuder, Smith, Koornneef, & Kendrick, 2000) were only present in the *irPhyB1-B2-150-6* line (Figure S1g).

Although *irCry2* plants showed a small reduction in *NaCry1* transcript accumulations compared with EV plants, the constructs designed for both *irCry2* and *irPhyB1-B2* lines (Table S1) did not show any off-target sites when the sequence fragments used for the transformation constructs were blasted against the entire *N. attenuata* genome (Xu et al., 2017). From this, we infer that any nonspecific effects of the constructs result from possible coregulation among the members within the same gene family.

3.3 | Root-*PhyB1B2* expression and signalling influence shoot growth of *N. attenuata* plants

Given that the graft junctions the region of the transmission of transgenes (Fuentes, Stegemann, Golczyk, Karcher, & Bock, 2014) is exposed to variable amounts of light under natural conditions, and for which photomorphogenic response of plastid greening provides a reasonable proxy (Melnyk & Meyerowitz, 2015), it was essential to first evaluate the stability of gene silencing across the graft junction in micrografted plants as they mature to know if this technique is useful for the study of root-expressed photoreceptor functions in real-world grown plants. To evaluate the stability of gene silencing in the graft junctions of micrografted plants, we micrografted control EV shoots onto roots silenced in *NaCAD* (*irCAD*, cinnamyl alcohol dehydrogenase) expression (Figure 2a). *CAD*-silencing results in red-stained cell walls undergoing the lignification process, which in *N. attenuata* occurs first in the stems and roots of the root/shoot junction, spreading upwards through the stem and downward through the roots as plants mature and are exposed to various stresses (Kaur et al., 2012). As such, micrografted EV/*irCAD* plants provide a useful tool to visually examine the stability of gene-silencing at the graft junction in plants grown under a variety of conditions. Seven to 10 day-old EV and *irCAD* seedlings were grafted (Fragoso et al., 2011) to create heterografts (EV/*irCAD*, shoots/roots) and control homografts (EV/EV or *irCAD*/*irCAD*), which were planted into soil and grown into mature plants under a variety of conditions. Tissues surrounding the graft junction of 41 day-old EV/EV, EV/*irCAD*, and *irCAD*/*irCAD* grafts were sliced into 1-mm-thick slices to evaluate the red pigmentation of the vascular tissues of stems and roots, as well as the accumulation of *NaCAD* transcripts, as quantified by qPCR (Figure 2a). The red pigmentation and the reduction in *NaCAD* transcript levels were confined to the graft junction area and to the belowground, but not aboveground, portions of EV/*irCAD* grafts (Figure 2a), results which are consistent with the more coarse-grained analysis of a previous study (Fragoso et al., 2011) that demonstrated that when the silenced lines are used as rootstocks, the silencing of the target genes is restricted to the roots of heterografted plants. From these data, we infer that the micrografting technique is a robust tool to create plants with "blind" roots to study photoreceptor function in field-grown *N. attenuata* plants.

Next, we created heterografts combining EV shoots to roots consisting of the lines silenced in *NaPhyA* (*irPhyA*), or in *NaPhyB1* and *NaPhyB2* (*irPhyB1xB2* or *irPhyB1-B2*) or in *NaCry2* (*irCry2*) expression, to produce heterografts of EV/*irPhyA*, EV/*irPhyB1xB2* or EV/*irPhyB1-B2*, and EV/*irCry2*. Homografts of EV/EV, *irPhyA*/*irPhyA*, *irPhyB1xB2*/*irPhyB1xB2*, *irPhyB1-B2*/*irPhyB1-B2*, and *irCry2*/*irCry2* were used as controls. The silencing of the photoreceptor target gene(s) in the transgenic lines when used as scions or rootstocks of

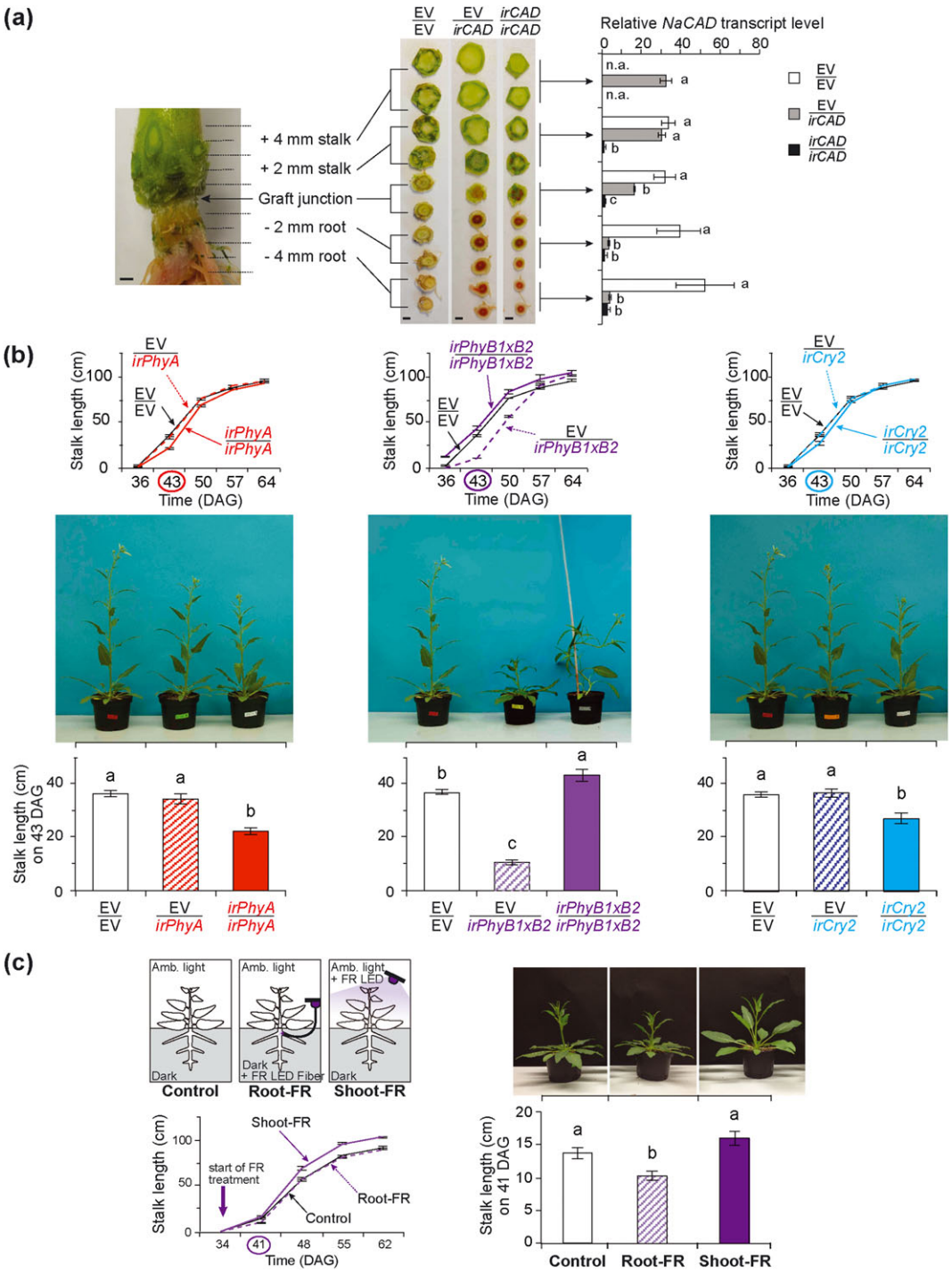

FIGURE 2 Root-expressed *NaPhyB1B2* mediate FR control of shoot growth of *N. attenuata* plants. (a) Red pigment, a visual marker of the silencing of *NaCAD* gene, and transcript accumulation in 1-mm cuts of the shoot-root junction area of 41-day-old EV/EV, EV/*irCAD*, and *irCAD*/*irCAD* grafts. Black scale bars in pictures represent 1 mm. Bars indicate *EF1a*-normalized relative transcript abundances of target *NaCAD* gene ±SE (n = 4). Different letters indicate statistically significant differences determined by Student–Newman–Keuls test (p < .05). (b) Plant growth from vegetative to late reproductive stages (36–64 DAG) were compared between heterografts of EV shoots combined to *NaPhyA*-silenced (line *irPhyA*-200), *NaPhyB1B2*-silenced (line *irPhyB1xB2*, cross between *irPhyB1*-178 × *irPhyB2*-204 lines), or *NaCry2*-silenced (line *irCry2*-282) roots and control homografts of both wild type (EV/EV) and their respective whole-plant silenced lines, for *NaPhyA* (*irPhyA*/*irPhyA*), for *NaPhyB1B2* (*irPhyB1xB2*/*irPhyB1xB2*), or for *NaCry2* (*irCry2*/*irCry2*). Plant pictures and bar graphs showed in (b) depict phenotypes observed on 43 DAG. Data shown as mean ±SE (n = 10 plants). Different letters indicate statistically significant differences determined by analysis of variance followed by Fisher LSD test (p < .05). (c) Plants were supplemented with FR (720-nm light-emitting diodes) directed either to the top of the shoots (shoot-FR) or to the upper part of the roots with fibre optic cables (root-FR) with 16-hr light/8-hr dark photoperiods; shoot growth was compared with control WT nontreated plants. Plant pictures and bar graphs showed in (c) depict phenotypes observed on 41 DAG, 14 days after the start of FR treatment. Data shown as mean ±SE (n = 20 plants). Different letters indicate statistically significant differences determined by analysis of variance followed by Fisher LSD test (p < .05). DAG = days after germination [Colour figure can be viewed at wileyonlinelibrary.com]

homografts or as rootstocks of heterografts were unchanged from those observed in the intact nongrafted plants (Figures S1c,f and S4a–c; Fragoso et al., 2017), and the gene silencing in heterografts was confined to the roots.

To investigate the function of root-expressed photoreceptors in plant growth and development, rosette diameter, leaf morphology, leaf angle, and stalk elongation were measured in all graft combinations, from early rosette to the late flowering stages of growth. The most dramatically altered trait in the heterografts silenced for root photoreceptors compared with control EV/EV homografts was in stalk elongation (Two-way repeated measures ANOVA, Genotype: $p < .001$, Days: $p < .001$, Genotype × Days: $p < .001$, for all comparisons of EV/EV grafts versus both heterografts and homografts of *irPhyA* (*irPhyA*-200), *irPhyB1xB2* (*irPhyB1*-178 × *irPhyB2*-204) or *irCry2* (*irCry2*-282); Figure 2b). Although the rate of stalk elongation at 43 DAG was significantly different in all silenced homografts of *irPhyA*/*irPhyA*, *irPhyB1xB2*/*irPhyB1xB2*, and *irCry2*/*irCry2* grafts when compared with EV/EV, only the EV/*irPhyB1xB2*, but not the EV/*irPhyA* or the EV/*irCry2*, heterograft was significantly delayed in stalk elongation compared with EV/EV plants (Two-way repeated measures ANOVAs, followed by genotype comparisons within 43 DAG, time: EV/*irPhyA* vs. EV/EV, $p = .179$; EV/*irPhyB1xB2* vs. EV/EV, $p < .001$; EV/*irCry2* vs. EV/EV, $p = .238$; Figure 2b). To deepen the analysis, a second independent line of *irPhyA* (*irPhyA*-213), *irPhyB1xB2* (*irPhyB1*-246 × *irPhyB2*-171), and *irCry2* (*irCry2*-318) was also used, grafted, and monitored in parallel. Grafts of independently generated *irPhyA*, *irPhyB1xB2*, or *irCry2* lines showed stalk elongation rates that were indistinguishable from those observed in the first lines used (Figures 2b and S4d); and, consistently, only EV/*irPhyB1xB2* heterografts showed a significant delay in stalk elongation compared with EV/EV grafts (Two-way repeated measures ANOVA, followed by genotype comparisons within 43 DAG time: EV/*irPhyA* vs. EV/EV, $p = .292$; EV/*irPhyB1xB2* vs. EV/EV, $p < .001$; EV/*irCry2* vs. EV/EV, $p = .382$; Figure S4d). From these results, we conclude that the delayed stalk elongation phenotype of EV/*irPhyB1xB2* grafts resulted from the specific silencing of root-expressed *NaPhyB1* and *NaPhyB2*.

3.4 | Root-PhyB1B2 is regulated by far-red light and control shoot growth of *N. attenuata* plants

To determine whether the delayed stalk elongation phenotype of EV/*irPhyB1xB2* grafts could be phenocopied by light-induced inactivation of root- or shoot-PHY proteins, we supplemented nongrafted EV plants with FR (LEDs emitting light at 720 nm; fluence rate: ≈80 $\mu mol \cdot m^{-2} \cdot s^{-1}$ at 1-cm distance from the lens). Rosette-stage (8-cm diameter), wild-type plants grown in 1-L soil-containing pots were exposed to FR either to the entire shoots (shoot-FR, Figure S2) or to a localized 5-mm^2 area at the upper part of the primary roots, just below the soil surface (root-FR, Figure S2). The FR LED source was the same for both shoot and root treatments (5 W), however, fibre optic cables (transmission efficiency >95%) provided the root-FR supplementation. FR was supplemented for the duration of the light period (06:00–22:00 hr) for both shoot- or root-FR supplementations. Shoot-FR plants resembled intact hemizigous *irPhyB1xB2* plants growing under control light conditions, and homografts of *irPhyB1xB2*/*irPhyB1xB2*, with their characteristic hyponastic and slender leaves and accelerated stalk elongations (Figure 2c). Root-FR plants resembled EV/*irPhyB1xB2* grafts and were delayed in stalk elongation compared with control nontreated plants (on 41 DAG and after 2 weeks of FR treatment, $p < .05$; Figure 2c). The delayed stalk elongation of root-FR plants compared with control non-FR plants was mild and transient, and restricted to the early stages of vegetative development. In comparison with the strong and persistent delay in stalk elongation found in EV/*irPhyB1xB2*, the effect of the root-FR supplementation of EV plants was decidedly weaker and transient, likely due to the fact that the FR supplementation was applied to a single location of the primary roots of 34-week-old plants, and this inactivation of PhyB1B2 was likely much less than that of the endogenously silenced plants, which had their PhyB1B2 functions in the entire root systems inactivated since germination. Overall, the data are consistent with the hypothesis that root-*NaPhyB1* and -*NaPhyB2* regulate light-dependent signalling, especially R/FR signalling, which plays a role in regulating shoot growth of *N. attenuata* plants.

3.5 | Root-*HY5* and hormone homeostasis are regulated by root-expressed *PhyB1B2*

Recently, Lee et al. (2016) demonstrated that root-phytochrome B is directly activated by stem-piped light to induce *HY5* expression that modulates root gravitropism in Arabidopsis seedlings. In order to evaluate if a similar signalling system operates in the roots of adult *N. attenuata* plants, we measured *NaHY5* transcript levels in the leaves and roots of plants subjected to aboveground light manipulations (Figure 3a). Eight hours dark-adapted wild-type *N. attenuata* plants on 35 DAG had their shoots exposed to light for an hour (from 6:00 to 7:00 hr), whereas control plants remained in the dark for the same time period. Light-exposed leaves showed a 15.8-fold increase in *NaHY5* transcripts compared with dark-adapted leaves (Figure 3a). Although the roots of plants of both light- and dark-treated leaves were both in the dark in the sand, the roots of light-exposed plants showed a 2.3-fold increase in *NaHY5* transcript accumulations compared with the roots of plants kept in the dark.

To investigate whether *NaHY5* is involved in the root-*NaPhyB1B2*-mediated delay in stalk elongation, we examined *NaHY5* transcript accumulation in the leaves and roots of EV/*irPhyB1xB2* grafts and control homografts of EV/EV and *irPhyB1xB2*/*irPhyB1xB2*, all grown under natural shoot-light and root-dark conditions (Figure 3b). *NaHY5* transcript accumulations were strongly suppressed in the roots of both EV/*irPhyB1xB2* and *irPhyB1xB2*/*irPhyB1xB2* grafts when compared with those of EV/EV grafts. In addition, leaves of EV/*irPhyB1xB2* grafts also showed a reduction in *NaHY5* transcript accumulation when compared with leaves of EV/EV grafts (Figure 3b), consistent with the notion that root- and shoot-expressed *HY5* are coregulated (Chen et al., 2016). Moreover, *NaHY5* transcript accumulation of roots and leaves of shoot- or root-FR-treated plants compared with those of nontreated control plants showed a trend of reduced *NaHY5* transcript accumulations when compared with nontreated control plants; however, the difference was not statistically significant ($p = .158$; Figure 3c), which is consistent with the transient and mild growth phenotype observed in root-FR-treated plants

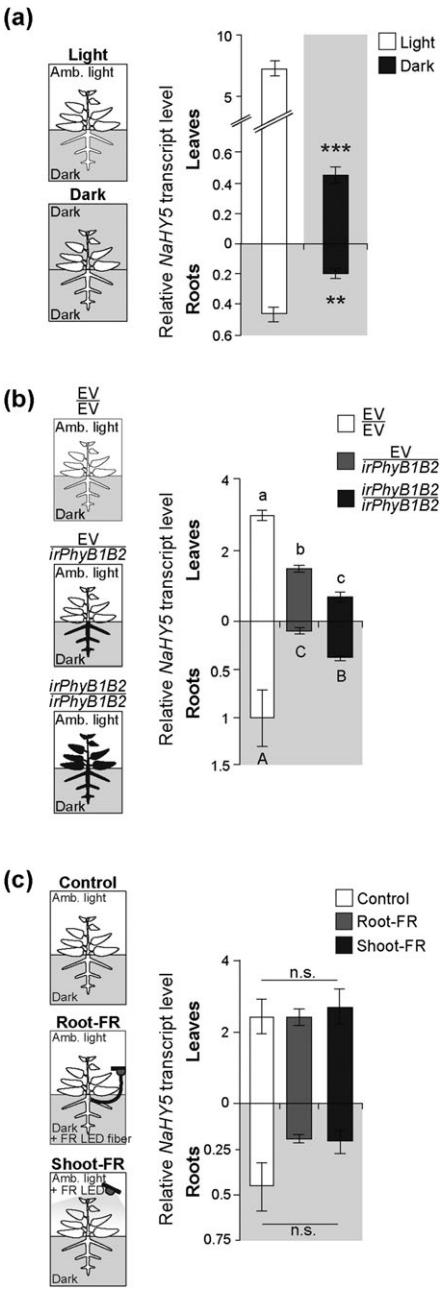

FIGURE 3 Transcriptional activation of root-*HY5* by aboveground ambient light requires root expressed *NaPhyB1B2* and is suppressed by root-FR exposure. (a) Transcript abundance of *HY5* was measured in shoots and roots of dark-acclimated plants followed by 1 hr of shoot light exposure (Light), whereas control plants remained for the same time in the dark (Dark). Bars indicate *EF1a*-normalized relative transcript abundances of target genes ±SE (n = 6 plants). Asterisks indicate statistically significant differences determined by Student's t test (***p < .001) for the leaf samples or by Mann–Whitney Rank Sum test (**p = .004) for the root samples. Transcript abundance of *HY5* was measured in plants with (b) *NaPhyB1B2*-silenced roots (EV/*irPhyB1xB2*) and in control homografts (EV/EV and *irPhyB1xB2*/*irPhyB1xB2*) and (c) in plants supplemented with FR either to shoots (shoot-FR) or roots (root-FR), whereas control plants remained under ambient light. Bars indicate *EF1a*-normalized relative transcript abundances of target genes ±SE (n = 4 plants). Different letters indicate statistically significant differences determined by Student–Newman–Keuls test for the root samples and by Fisher LSD test for the leaf samples (p < .05). All plants were grown under the same light/dark cycles in climate chambers (a) or in glasshouse (b and c)

(Figure 2c). Overall, these data suggest that root-PhyB1B2 is required for light-induced transcriptional activation of *HY5* in *N. attenuata* plants.

Light-responsive HY5 is also known to promote photomorphogenesis by modulating the biosynthesis and signalling pathways of phytohormones such as gibberellic acids, auxin, abscisic acid, and cytokinins (Alabadí et al., 2008; Chen et al., 2008; Lee et al., 2007; Moriwaki, Miyazawa, Fujii, & Takahashi, 2012; Novák et al., 2014; Sibout et al., 2006). Individual phytohormone homeostasis and phytohormone crosstalk are essential for regulating growth and development in plants and, when disrupted, dramatic phenotypic changes result (Jones et al., 2010; Kurepin & Pharis, 2014; Mravec et al., 2009; Tanaka et al., 2005). EV/*irPhyB1xB2* plants had significantly elevated phytohormones such as gibberellic acids, auxins, cytokinins, and abscisic acid in all tissues analysed (i.e., stalk, leaves, and roots) when compared with those of EV/EV and *irPhyB1xB2*/*irPhyB1xB2* control homografts (Figure S5). Although clearly more work is required to understand the intricate and dynamic mechanisms by which disrupted HY5 transcription and hormone homeostasis leads to differences in plant growth when roots are "blind," the results presented here demonstrate the robustness of the whole-plant growth consequences of this light-mediated systemic plant signalling.

3.6 | The ecological function of root-PhyB1PhyB2 in shoot growth of *N. attenuata* plants

Recently, it has been demonstrated how light could reach and activate root-phytochrome B of Arabidopsis at molecular biology level (Lee et al., 2016), and also identified and characterized that *N. attenuata* plants have two copies of phytochrome B, *NaPhyB1*, and *NaPhyB2*, commonly found in Solanaceae species (Pratt et al., 1997; Pratt, Cordonnier-Pratt, Hauser, & Caboche, 1995), and that they act synergistically in the control of leaf development, and antagonistically in the control of flowering time (Fragoso et al., 2017). However, it still remains largely unexplored whether the root-specific role of phytochromes in plants contributes to such traits.

In this study, we demonstrate how *PhyB1B2* and *HY5* gene expression and the ambient light from aboveground and FR-light applied to roots influence growth and development of plants. Importantly, to investigate the function of root-*NaPhyB1* and *NaPhyB2* under the conditions found in nature, we planted grafts with *NaPhyB1B2*-silenced roots (EV/*irPhyB1-B2*) EV grafts/EV grafts in a paired design in a field plot in *N. attenuata*'s native habitat, the Great Basin Desert, Utah, USA (Figure 4a), and monitored their growth and development in two independent field seasons, 2012 and 2013. The silencing of *NaPhyB1* and *NaPhyB2* was confined to the roots of field-grown EV/*irPhyB1-B2* plants (Figure S6). Consistent with the glasshouse results of EV/*irPhyB1xB2* (Figure 2b), field-grown EV/*irPhyB1-B2* grafts were delayed in stalk elongation compared with EV/EV grafts consistently in two independent field seasons (Two-way repeated measures ANOVA, followed by Fisher LSD test, Genotype: p = .05, Days: p < .001, Genotype × Days: p = .043, n = 20 plants for the 2012 field experiment; Genotype: p = .078, Days: p < .001, Genotype × Days: p = .093, n = 12 plants for the 2013 field experiment; Figure 4b). The lower replicate number in the 2013 field

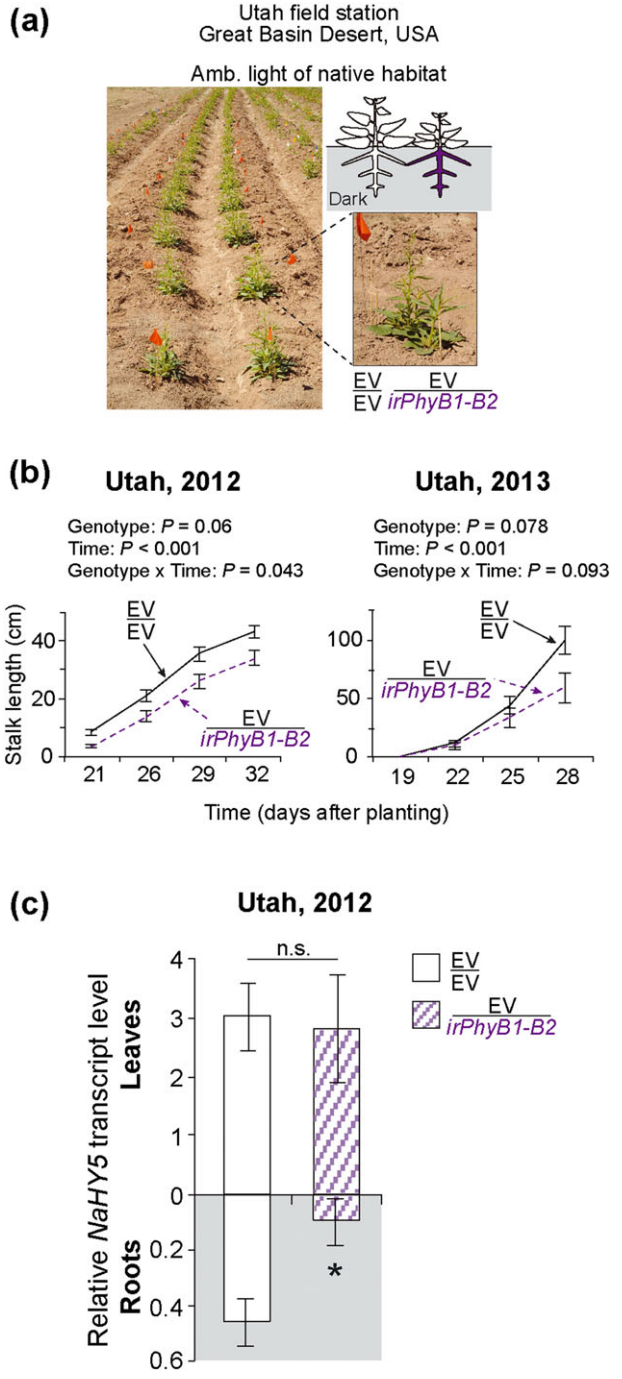

FIGURE 4 In nature, plants with *NaPhyB1B2*-silenced roots (EV/*irPhyB1-B2*) were delayed in stalk elongation compared with EV/EV control plants. EV/EV and EV/*irPhyB1-B2* plants were planted in a size-matched paired design in a field plot in the Great Basin Desert, Utah, USA, (a) and their growth was monitored in two independent field seasons of 2012 and 2013 (b). Data shown are mean ±SE (n = 20 plants for Utah 2012 and n = 12 plants for Utah 2013), and statistically significant differences were determined by two-way repeated-measures analysis of variance followed by Fisher LSD test (Genotype: p = .006 for Utah 2012 and p = .078 for Utah 2013, Days: p < .001 for both years, Genotype × Days: p = .043 for Utah 2012 and p = .093 for Utah 2013). Relative transcript abundance of *HY5* was measured in both leaf and root samples of field -grown EV/EV and EV/*irPhyB1-B2* plants, Utah 2012 (c). Bars indicate *EF1a*-normalized relative transcript abundances of target genes ±SE (n = 6 plants). Asterisks indicate statistically significant differences determined by Student's t test (p < .05) [Colour figure can be viewed at wileyonlinelibrary.com]

experiment likely accounts for the marginally significant effect found in this year. In addition, and again consistent with the glasshouse-grown EV/*irPhyB1xB2* plants, roots of field-grown EV/*irPhyB1-B2* accumulated lower levels of *NaHY5* transcripts when compared with roots of field-grown EV/EV plants (Student's t-test p < .05; Figure 4c).

Consistent with results reported from *N. attenuata* and other plant species (Devlin, Halliday, Harberd, & Whitelam, 1996; Fragoso et al., 2017; Halliday, Koornneef, & Whitelam, 1994; Sheehan, Kennedy, Costich, & Brutnell, 2007; Takano et al., 2005; Weller et al., 2000), plants silenced for *NaPhyB1* and *NaPhyB2* in both shoots and roots (*irPhyB1xB2*/*irPhyB1xB2* and *irPhyB1-B2*/*irPhyB1-B2*) showed accelerated stalk elongation compared with those of EV/EV grafts (Figures 2b and S1g). However, plants silenced for *NaPhyB1* and *NaPhyB2* only in the roots (EV/*irPhyB1xB2* and EV/*irPhyB1-B2*) showed delayed stalk elongation compared with EV/EV control grafts, both in controlled glasshouse conditions, where plants were grown in pots and under artificial light (Figure 2), and in real-world conditions found in nature (Figure 4). In this study, we showed that plants with "sighted" shoots and "blind" roots display completely different growth patterns from those of plants with both "sighted" shoot and roots in both growth conditions (Figures 2 and 4), and demonstrated that roots integrate the environmental information and contribute to critical life history traits such as the timing of resource allocations to stalk elongation.

In addition to day-length changes perceived by photoreceptors, it is widely accepted that the temperature is also a critical determinant of the timing of flowering in plants (Song, Ito, & Imaizumi, 2013). Recently, the function of phytochromes in the shade avoidance syndrome were shown to be temperature-dependent (Patel et al., 2013), and that phytochromes are not only light sensing photoreceptors but also temperature sensing thermosensors (Jung et al., 2016). AtPhyB directly binds to promoters of temperature-responsive genes in a temperature-dependent manner and integrates temperature information to regulate growth and development. A potential temperature-sensing function of phytochromes is also consistent with our glasshouse experiments: the delayed shoot elongation phenotype of EV/*irPhyB1xB2* grafts compared with EV/EV plants was much stronger when plants were grown in the summer season compared with the winter season. In general, we observed that shoot elongation in the winter was delayed when compared with plants of the same age grown in the summer season, but this difference was much larger in EV/EV plants compared with those of EV/*irPhyB1xB2* plants: 80% and 56% shorter stalk lengths in winter compared with those in summer, respectively (Figure S7). Although plants were grown in a temperature-controlled glasshouse, the maximum ambient day-time air temperatures (and hence soil pot temperatures) during the summer season is much higher than those of the winter season, due to the additional summer natural sunlight that enhances to the glasshouse temperature fluctuations (daily temperature maxima: 31 vs. 25 °C in summer and winter, respectively). Several studies have shown that crosstalk among light and temperature signals mediates elongation and flower times (reviewed in (Franklin et al., 2014). Temperature either synergistically or antagonistically interacts with light irradiance to influence stalk elongation (Bours, Kohlen, Bouwmeester, & van der Krol, 2015; Franklin, 2009; Gangappa & Kumar, 2017; Karayekov,

Sellaro, Legris, Yanovsky, & Casal, 2013). We hypothesize that root-PhyB1B2 function not only as light sensors but also as thermosensors to modulate the rate at which stalks elongate in *N. attenuata* plants. As *N. attenuata* is a desert plant, which flowers when ambient air temperatures are well above 40 °C and soil temperature profiles reflect water availability, we speculate that root-PhyB1B2 sense light and temperature to optimize shoot growth and/or flowering time to a plant's particular location.

3.7 | CONCLUSIONS

Our study provides compelling evidence how a disrupted light perception in the roots affects target downstream gene expression, hormone homeostasis, and optimal plant growth. We show that root-expressed PhyB1B2 is sensing aboveground light information and plays an important role not only as establishing root initiations in seedlings but also as regulators of shoot growth of mature adult plants. These effects were observed in glasshouse and, most importantly, confirmed during two years of field work in the plant's native habitat. However, challenging field experiments might be, studying the function of photoreceptors under natural conditions is necessary to understand a plant's evolved environmental responses. Real world experiments are essential if we are to appreciate how plants solve life's persistent light-driven questions.

ACKNOWLEDGMENTS

We thank A. Block for help in analysing transcript abundant of phytochromes in EV and *irPhy* grafts; D. Veit for building LED devices for FR experiments; D. Kessler, C. Diezel, and E. Rothe for field planting and preparation; F. Yon, A. Weinhold, G. Lee, and E. Rothe for help in glasshouse and field sampling; and Brigham Young University for the use of their Lytle Ranch Preserve field station. This work is supported by European Research Council advanced grant ClockworkGreen (293926) to ITB, the Global Research Lab program (2012055546) from the National Research Foundation of Korea, the Max Planck Society and particularly, the Human Frontier Science Program (RGP0002/2012). The authors declare no conflicts of interest.

AUTHOR CONTRIBUTIONS

Conceived and designed experiments: Y. Oh and V. Fragoso, S-G. Kim, C-M. Park, and I.T. Baldwin. Performed experiments: Y. Oh, V. Fragoso, I.T. Baldwin, and F. Guzzonato. Analysed data: Y. Oh and V. Fragoso. Wrote manuscript: Y. Oh and V. Fragoso and I.T. Baldwin.

ORCID

Ian T. Baldwin http://orcid.org/0000-0001-5371-2974

REFERENCES

Adam, E., Kozma-Bognar, L., Schafer, E., & Nagy, F. (1997). Tobacco phytochromes: Genes, structure and expression. *Plant, Cell and Environment*, *20*, 678–684.

Alabadí, D., Gallego-Bartolomé, J., Orlando, L., García-Cárcel, L., Rubio, V., Martínez, C., … Blázquez, M. A. (2008). Gibberellins modulate light signaling pathways to prevent Arabidopsis seedling de-etiolation in darkness. *Plant Journal*, *53*, 324–335.

Bae, G., & Choi, G. (2008). Decoding of light signals by plant phytochromes and their interacting proteins. *Annual Review of Plant Biology*, *59*, 281–311.

Bours, R., Kohlen, W., Bouwmeester, H. J., & van der Krol, A. (2015). Thermoperiodic control of hypocotyl elongation depends on auxin-induced ethylene signaling that controls downstream phytochrome interacting factor 3 activity. *Plant Physiology*, *167*, 517–530.

Blázquez, M. A., Ahn, J. H., & Weigel, D. (2003). A thermosensory pathway controlling flowering time in Arabidopsis thaliana. *Nature Genetics*, *33*, 168–171.

Brachi, B., Faure, N., Horton, M., Flahauw, E., Vazquez, A., Nordborg, M., … Roux, F. (2010). Linkage and association mapping of *Arabidopsis thaliana* flowering time in nature. *PLoS Genetics*, *6*, 40.

Casal, J. J. (2013). Photoreceptor signaling networks in plant responses to shade. *Annual Review of Plant Biology*, *64*, 403–427.

Chen, H., Zhang, J., Neff, M. M., Hong, S.-W., Zhang, H., Deng, X.-W., & Xiong, L. (2008). Integration of light and abscisic acid signaling during seed germination and early seedling development. *Proceedings of the National Academy of Sciences of the United States of America*, *105*, 4495–4500.

Chen, X., Yao, Q., Gao, X., Jiang, C., Harberd, N. P., & Fu, X. (2016). Shoot-to-root mobile transcription factor HY5 coordinates plant carbon and nitrogen acquisition. *Current Biology*, *26*, 640–646.

Christie, J. M., Blackwood, L., Petersen, J., & Sullivan, S. (2015). Plant flavoprotein photoreceptors. *Plant and Cell Physiology*, *56*, 401–413.

Ciani, A., Goss, K.-U., & Schwarzenbach, R. P. (2005). Light penetration in soil and particulate minerals. *European Journal of Soil Science*, *56*, 561–574.

Clack, T., Mathews, S., & Sharrock, R. A. (1994). The phytochrome apoprotein family in Arabidopsis is encoded by five genes: The sequences and expression of PHYD and PHYE. *Plant Molecular Biology*, *25*, 413–427.

Cluis, C. P., Mouchel, C. F., & Hardtke, C. S. (2004). The *Arabidopsis* transcription factor HY5 integrates light and hormone signaling pathways. *The Plant Journal*, *38*, 332–347.

Correll, M. J., & Kiss, J. Z. (2005). The roles of phytochromes in elongation and gravitropism of roots. *Plant and Cell Physiology*, *46*, 317–323.

Costigan, S. E., Warnasooriya, S. N., Humphries, B. A., & Montgomery, B. L. (2011). Root-localized phytochrome chromophore synthesis is required for photoregulation of root elongation and impacts root sensitivity to jasmonic acid in Arabidopsis. *Plant Physiology*, *157*, 1138–1150.

De Simone, S., Oka, Y., & Inoue, Y. (2000). Effect of light on root hair formation in *Arabidopsis thaliana* phytochrome-deficient mutants. *Journal of Plant Research*, *113*, 63–69.

Devlin, P. F., Halliday, K. J., Harberd, N. P., & Whitelam, G. C. (1996). The rosette habit of *Arabidopsis thaliana* is dependent upon phytochrome action: Novel phytochromes control internode elongation and flowering time. *The Plant Journal*, *10*, 1127–1134.

Devlin, P. F., Robson, P. R., Patel, S. R., Goosey, L., Sharrock, R. A., & Whitelam, G. C. (1999). Phytochrome D acts in the shade-avoidance syndrome in Arabidopsis by controlling elongation growth and flowering time. *Plant Physiology*, *119*, 909–915.

Dyachok, J., Zhu, L., Liao, F., He, J., Huq, E., & Blancaflor, E. B. (2011). SCAR mediates light-induced root elongation in Arabidopsis through photoreceptors and proteasomes. *The Plant Cell*, *23*, 3610–3626.

Endo, M., Araki, T., & Nagatani, A. (2016). Tissue-specific regulation of flowering by photoreceptors. *Cellular and Molecular Life Sciences*, *73*, 829–839.

Fitter, A. H., & Fitter, R. S. R. (2002). Rapid changes in flowering time in British plants. *Science*, *296*, 1689–1691.

Fragoso, V., Goddard, H., Baldwin, I. T., & Kim, S.-G. (2011). A simple and efficient micrografting method for stably transformed Nicotiana attenuata plants to examine shoot-root signaling. *Plant Methods*, *7*, 34.

Fragoso, V., Oh, Y., Kim, S.-G., Gase, K., & Baldwin, I. T. (2017). Functional specialization of *Nicotiana attenuata* phytochromes in leaf

development and flowering time. *Journal of Integrative Plant Biology*, *59*, 205–224.

Franklin, K. A. (2009). Light and temperature signal crosstalk in plant development. *Current Opinion in Plant Biology*, *12*, 63–68.

Franklin, K. A., & Quail, P. H. (2010). Phytochrome functions in Arabidopsis development. *Journal of Experimental Botany*, *61*, 11–24.

Franklin, K. a., Toledo-Ortiz, G., Pyott, D. E., & Halliday, K. J. (2014). Interaction of light and temperature signalling. *Journal of Experimental Botany*, *65*, 2859–2871.

Fuentes, I., Stegemann, S., Golczyk, H., Karcher, D., & Bock, R. (2014). Horizontal genome transfer as an asexual path to the formation of new species. *Nature*, *511*, 232–235.

Galvão, V. C., & Fankhauser, C. (2015). Sensing the light environment in plants: Photoreceptors and early signaling steps. *Current Opinion in Neurobiology*, *34*, 46–53.

Gangappa, S. N., & Kumar, S. V. (2017). DET1 and HY5 control PIF4-mediated thermosensory elongation growth through distinct mechanisms. *Cell Reports*, *18*, 344–351.

Gase, K., & Baldwin, I. T. (2012). Transformational tools for next-generation plant ecology: Manipulation of gene expression for the functional analysis of genes. *Plant Ecology & Diversity*, *5*, 485–490.

Gase, K., Weinhold, A., Bozorov, T., Schuck, S., & Baldwin, I. T. (2011). Efficient screening of transgenic plant lines for ecological research. *Molecular Ecology Resources*, *11*, 890–902.

Goosey, L., Palecanda, L., & Sharrock, R. A. (1997). Differential patterns of expression of the Arabidopsis PHYB, PHYD, and PHYE phytochrome genes. *Plant Physiology*, *115*, 959–969.

Halliday, K. J., Koornneef, M., & Whitelam, G. C. (1994). Phytochrome B and at least one other phytochrome mediate the accelerated flowering response of *Arabidopsis thaliana L.* to low red/far-red ratio. *Plant Physiology*, *104*, 1311–1315.

Jones, B., Gunnerås, S. A., Petersson, S. V., Tarkowski, P., Graham, N., May, S., … Ljung, K. (2010). Cytokinin regulation of auxin synthesis in Arabidopsis involves a homeostatic feedback loop regulated via auxin and cytokinin signal transduction. *The Plant Cell*, *22*, 2956–2969.

Jung, J.-H., Domijan, M., Klose, C., Biswas, S., Ezer, D., Gao, M., … Wigge, P. A. (2016). Phytochromes function as thermosensors in Arabidopsis. *Science*, *354*, 886–889.

Karayekov, E., Sellaro, R., Legris, M., Yanovsky, M. J., & Casal, J. J. (2013). Heat shock-induced fluctuations in clock and light signaling enhance phytochrome B-mediated Arabidopsis deetiolation. *The Plant Cell*, *25*, 2892–2906.

Kaur, H., Shaker, K., Heinzel, N., Ralph, J., Galis, I., & Baldwin, I. T. (2012). Environmental stresses of field growth allow cinnamyl alcohol dehydrogenase-deficient *Nicotiana attenuata* plants to compensate for their structural deficiencies. *Plant Physiology*, *159*, 1545–1570.

Krügel, T., Lim, M., Gase, K., Halitschke, R., & Baldwin, I. T. (2002). Agrobacterium-mediated transformation of *Nicotiana attenuata*, a model ecological expression system. *Chemoecology*, *12*, 177–183.

Kurepin, L. V., & Pharis, R. P. (2014). Light signaling and the phytohormonal regulation of shoot growth. *Plant Science*, *229*, 280–289.

Lau, O. S., & Deng, X. W. (2010). Plant hormone signaling lightens up: Integrators of light and hormones. *Current Opinion in Plant Biology*, *13*, 571–577.

Lee, H., Ha, J., Kim, S., Choi, H., Kim, Z. H., Han, Y., … Park, C. (2016). Stem-piped light activates phytochrome B to trigger light responses in *Arabidopsis thaliana* roots. *Science Signaling*, *9*, ra106.

Lee, H.-J., Park, Y.-J., Ha, J.-H., Baldwin, I. T., & Park, C.-M. (2017). Multiple routes of light signaling during root photomorphogenesis. *Trends in Plant Science*, *22*, 803–812.

Lee, J., He, K., Stolc, V., Lee, H., Figueroa, P., Gao, Y., … Deng, X. W. (2007). Analysis of transcription factor HY5 genomic binding sites revealed its hierarchical role in light regulation of development. *The Plant Cell Online*, *19*, 731–749.

Legris, M., Klose, C., Costigliolo, C., Burgie, E., Neme, M., Hiltbrunner, A., … Casal, J. J. (2016). Phytochrome B integrates light and temperature signals in Arabidopsis. *Science*, *354*, 897–900.

Lekberg, Y., & Helgason, T. (2018). In situ mycorrhizal function—Knowledge gaps and future directions. *The New Phytologist*. https://doi.org/10.1111/nph.15064

Lumsden, P. J. (2002) 15. *Photoperiodism in Plants*, Springer, Berlin, Heidelberg.

Mandoli, D. F., & Briggs, W. R. (1982). Optical properties of etiolated plant tissues. *Proceedings of the National Academy of Sciences of the United States of America*, *79*, 2902–2906.

Mandoli, D. F., Ford, G. a., Waldron, L. J., Nemson, J. a., & Briggs, W. R. (1990). Some spectral properties of several soil types: Implications for photomorphogenesis. *Plant, Cell and Environment*, *13*, 287–294.

Mathews, S., & Sharrock, R. A. (1997). Phytochrome gene diversity. *Plant Cell and Environment*, *20*, 666–671.

Melnyk, C. W., & Meyerowitz, E. M. (2015). Plant grafting. *Current Biology*, *25*, R183–R188.

Mo, M., Yokawa, K., Wan, Y., & Baluška, F. (2015). How and why do root apices sense light under the soil surface? *Frontiers in Plant Science*, *6*, 1–8.

Montgomery, B. L. (2016). Spatiotemporal phytochrome signaling during photomorphogenesis: From physiology to molecular mechanisms and back. *Frontiers in Plant Science*, *7*, 1–8.

Moriwaki, T., Miyazawa, Y., Fujii, N., & Takahashi, H. (2012). Light and abscisic acid signalling are integrated by MIZ1 gene expression and regulate hydrotropic response in roots of Arabidopsis thaliana. *Plant, Cell and Environment*, *35*, 1359–1368.

Mravec, J., Skůpa, P., Bailly, A., Hoyerová, K., Krecek, P., Bielach, A., … Friml, J. (2009). Subcellular homeostasis of phytohormone auxin is mediated by the ER-localized PIN5 transporter. *Nature*, *459*, 1136–1140.

Nimmo, H. G. (2018). Entrainment of Arabidopsis roots to the light:Dark cycle by light piping. *Plant, Cell & Environment*, 1–7.

Novák, J., Černý, M., Pavlů, J., Zemánková, J., Skalák, J., Plačková, L., & Brzobohatý, B. (2014). Roles of proteome dynamics and cytokinin signaling in root to hypocotyl ratio changes induced by shading roots of arabidopsis seedlings. *Plant and Cell Physiology*, *56*, 1006–1018.

Patel, D., Basu, M., Hayes, S., Majláth, I., Hetherington, F. M., Tschaplinski, T. J., & Franklin, K. a. (2013). Temperature-dependent shade avoidance involves the receptor-like kinase ERECTA. *Plant Journal*, *73*, 980–992.

Poorter, H., Fiorani, F., Pieruschka, R., Wojciechowski, T., van der Putten, W. H., Kleyer, M., … Postma, J. (2016). Pampered inside, pestered outside? Differences and similarities between plants growing in controlled conditions and in the field. *New Phytologist*, *212*, 838–855.

Pratt, L. H., Cordonnier-Pratt, M. M., Hauser, B., & Caboche, M. (1995). Tomato contains two differentially expressed genes encoding B-type phytochromes, neither of which can be considered an ortholog of Arabidopsis phytochrome B. *Planta*, *197*, 203–206.

Pratt, L. H., Cordonnier-Pratt, M.-M., Kelmenson, P. M., Lazarova, G. I., Kubota, T., & Alba, R. M. (1997). The phytochrome gene family in tomato (*Solanum lycopersicum L.*). *Plant, Cell and Environment*, *Chichester*, *20*, 672–677.

Reed, J. W., Nagpal, P., Poole, D. S., Furuya, M., & Chory, J. (1993). Mutations in the gene for the red/far-red light receptor phytochrome B alter cell elongation and physiological responses throughout Arabidopsis development. *The Plant Cell*, *5*, 147–157.

Salisbury, F. J., Hall, A., Grierson, C. S., & Halliday, K. J. (2007). Phytochrome coordinates Arabidopsis shoot and root development. *Plant Journal*, *50*, 429–438.

Sharrock, R. A. (2002). Patterns of expression and normalized levels of the five Arabidopsis phytochromes. *Plant Physiology*, *130*, 442–456.

Sheehan, M. J., Kennedy, L. M., Costich, D. E., & Brutnell, T. P. (2007). Subfunctionalization of PhyB1 and PhyB2 in the control of seedling and mature plant traits in maize. *The Plant Journal*, *49*, 338–353.

Sibout, R., Sukumar, P., Hettiarachchi, C., Holm, M., Muday, G. K., & Hardtke, C. S. (2006). Opposite root growth phenotypes of hy5 versus hy5 hyh mutants correlate with increased constitutive auxin signaling. *PLoS Genetics*, *2*, 1898–1911.

Somers, D. E., & Quail, P. H. (1995a). Temporal and spatial expression patterns of PHYA and PHYB genes in Arabidopsis. *The Plant Journal : For Cell and Molecular Biology*, *7*, 413–427.

Somers, D. E., & Quail, P. H. (1995b). Phytochrome-mediated light regulation of PHYA- and PHYB-GUS transgenes in *Arabidopsis thaliana* Seedlings. *Plant Physiology*, *107*, 523–534.

Song, Y. H., Ito, S., & Imaizumi, T. (2013). Flowering time regulation: Photoperiod- and temperature-sensing in leaves. *Trends in Plant Science*, *18*, 575–583.

Sun, Q., Yoda, K., & Suzuki, H. (2005). Internal axial light conduction in the stems and roots of herbaceous plants. *Journal of Experimental Botany*, *56*, 191–203.

Sun, Q., Yoda, K., Suzuki, M., & Suzuki, H. (2003). Vascular tissue in the stem and roots of woody plants can conduct light. *Journal of Experimental Botany*, *54*, 1627–1635.

Takano, M., Inagaki, N., Xie, X., Yuzurihara, N., Hihara, F., Ishizuka, T., … Shinomura, T. (2005). Distinct and cooperative functions of phytochromes A, B, and C in the control of deetiolation and flowering in rice. *The Plant Cell*, *17*, 3311–3325.

Tanaka, K., Asami, T., Yoshida, S., Nakamura, Y., Matsuo, T., & Okamoto, S. (2005). Brassinosteroid homeostasis in Arabidopsis is ensured by feedback expressions of multiple genes involved in its metabolism. *Plant Physiology*, *138*, 1117–1125.

Tester, M., & Morris, C. (1987). The penetration of light through soil. *Plant Cell and Environment*, *10*, 281–286.

Tossi, V., Lamattina, L., Jenkins, G. I., & Cassia, R. O. (2014). Ultraviolet-B-induced stomatal closure in Arabidopsis is regulated by the UV RESISTANCE LOCUS8 photoreceptor in a nitric oxide-dependent mechanism. *Plant Physiology*, *164*, 2220–2230.

Weller, J. L., Schreuder, M. E. L., Smith, H., Koornneef, M., & Kendrick, R. E. (2000). Physiological interactions of phytochromes A, B1 and B2 in the control of development in tomato. *Plant Journal*, *24*, 345–356.

Xu, S., Brockmöller, T., Navarro-Quezada, A., Kuhl, H., Gase, K., Ling, Z., … Baldwin, I. T. (2017). Wild tobacco genomes reveal the evolution of nicotine biosynthesis. *Proceedings of the National Academy of Sciences*, *114*, 6133–6138.

Xu, W., Ding, G., Yokawa, K., Baluška, F., Li, Q. F., Liu, Y., … Zhang, J. (2013). An improved agar-plate method for studying root growth and response of *Arabidopsis thaliana*. *Scientific Reports*, *3*, 1–7.

Yokawa, K., Fasano, R., Kagenishi, T., & Baluška, F. (2014). Light as stress factor to plant roots—Case of root halotropism. *Frontiers in Plant Science*, *5*, 1–9.

SUPPORTING INFORMATION

Additional supporting information may be found online in the Supporting Information section at the end of the article.

How to cite this article: Oh Y, Fragoso V, Guzzonato F, Kim S-G, Park C-M, Baldwin IT. Root-expressed phytochromes B1 and B2, but not PhyA and Cry2, regulate shoot growth in nature. *Plant Cell Environ*. 2018;41:2577–2588. https://doi.org/10.1111/pce.13341